VTT Technical Research Centre of Finland

Spectroscopic methods for determination of latex content of coating layers

Kenttä, E.; Juvonen, K.; Halttunen, M.; Vyörykkä, J.

Published in:
Nordic Pulp and Paper Research Journal

Published: 01/12/2000

Document Version
Peer reviewed version

Spectroscopic methods for determination of latex content of coating layers

In Nordic Pulp & Paper Research Journal No 5, 2000 (15), p 579-585

Eija Kenttä, Kari Juvonen, Mari Halttunen, Jouko Vyörykkä

Keywords: Coated papers, Latex, Analysis , Infrared spectroscopy, Ultraviolet spectroscopy, Raman spectroscopy, Migration

SUMMARY:
IR Raman and UV methods were used to determine latex contents throughout different coating layers. The chosen methods have surface sensitivities from 1 to 8 micrometers, and the z-directional resolution of IR and Raman techniques is adjustable in the range of coating layer thickness. The ATR-IR, UV and confocal Raman microscope measurements gave, with certain limitations, latex contents of between 3 and 18 parts in clay and carbonate coatings. A study of calibration coatings showed how changes in coating pigments interfere with latex determination. Changes in pigment particle size and particle shape cause differences in signal intensity, especially in UV measurements. Clay in coatings gives rise to fluorescence, which interferes with Raman analyses. The results of these measurements will be used to give information on latex migration in coated papers.

Eija Kenttä and Kari Juvonen
Oy Keskuslaboratorio - Centrallaboratorium Ab (KCL)
P.O. Box 70, FIN-02151 Espoo, Finland
Mari Halttunen and Jouko Vyörykkä
Helsinki University of Technology, Laboratory of Forest Products Chemistry, P.O. Box 6300, FIN- 02150 Espoo, Finland

The main constituents in a coating layer are pigments and a binder, which is usually a latex and CMC or a combination of latex and starch. Uniform composition on the surface of the coating and throughout the coating layer in the z-direction is essential for good paper printing properties. Uneven latex distribution in the coating layer is often connected with mottling and surface strength problems (Engström, Rigdahl 1992, and Zang, Aspler, 1997).

Latex migration has been studied with surface-sensitive analytical methods like ESCA (electron spectroscopy for chemical analysis) and ATR-IR (attenuated total reflectance infrared) spectroscopy (Eklund et al. 1995, Zang, Aspler 1997, Kim et al. 1999). The surface distribution of SB latex has been analysed with an ultraviolet (UV) scanner (Kline et al. 1978, Engström et al. 1991). However, surface analysis does not give direct information on how the latex is distributed in the z-direction of the coating layer.

The z-directional latex distribution has been studied by stepwise scraping and surface analysis of the scraped coating (Tomimasu et al. 1986; Hattula, Aschan 1978). A new method based on elemental analysis by laser-induced plasma emission spectroscopy (LIPS) has also been used to measure binder/pigment ratio in the x-y and in z-directions of a coating layer (Häkkänen 1998, Zeyringer et al. 2000).

In photoacoustic spectroscopy (PAS) FTIR measurement, depth profiling is achieved by changing the modulation frequency. A higher modulation frequency gives spectral information from a thinner surface layer. In a

photoacoustic FTIR depth profile study of one-side coated paper, the phase modulation was changed from 100 Hz to 800 Hz (Wahls et al. 2000). PA spectra contained an increasing contribution from the base paper as the penetration depth changed from about 6.5 μm (at 800 Hz) to about 18.5 μm (at 100 Hz).

In the present study, four spectroscopic techniques were studied in terms of their ability to yield information on the latex distribution in successive layers a few micrometers in thickness through a coating. Surface-sensitive ATR-IR analysis was combined with a technique in which successive layers are ground off the coated paper surface.

Confocal Raman and PAS-FTIR both yield information from different depths in a non-destructive way. These techniques are widely used in the determination of depth profiles in multilayer polymer samples. However, there are few reports of their use to study the composition of coated paper. The development and the characteristics of confocal Raman profiling are described in detail elsewhere (Vyörykkä 1999). In the current study the confocal Raman and PAS-FTIR results from coating layers are compared with ATR-IR and UV measurements.

The advantage of using and comparing several techniques is that it gives more detailed and reliable estimates of the extent of composition variation in the coating layer.

Sample preparation

Coatings with different latex contents were prepared using two coating pigments: American clay (Hydragloss 90, J. M. Huber Corporation Engineered Materials) and ground carbonate (HC 90, Omya Oy), both of small particle size. The pigment compositions used were 100 parts clay, 50/50 parts clay/carbonate, 30/70 parts clay/carbonate and 100 parts carbonate. The content of styrenebutadiene (SB) latex (Dow DL 966, Tg 20°C) was varied from 3 to 18 parts. All coatings contained 1 part of CMC (Finnfix 10, Noviant Oy). The pH of the coating colors was adjusted to 8.5. The solids content of the coating colors was 61%.

The calibration coatings were applied on a glossy Mylar film. Coating colors containing clay were applied with a 90 μm slit rod, and the 100 parts carbonate coating color was applied with a 60 μm slit rod. The coatings were dried at room temperature. The dry coating layers were then released from the glossy plastic to be analysed on both surfaces.

Thin coating layers were applied using rods with slit widths between 10 and 60 μm. Coating layer thicknesses below 15 μm were applied with a 10 μm rod using diluted coating colors (solids content from 30% to 60%).

Coatings with different pigment sizes were applied on a rough Mylar film with a 90 μm rod. The rough Mylar film was used in this experiment because the dry coating layers were not released from the plastic. Only the upper surface of the coating was measured.

Three clay/latex and three carbonate/latex coatings were prepared. The chosen clay pigments, in decreasing order of particle size, were: Lithoprint , Hydragloss 90 and Hydragloss 92 (J. M. Huber Corporation Engineered Materials). The carbonate pigments, also in decreasing order of particle size, were: Hydrocarb 60, Hydrocarb 90 and Setacarb (Omya Oy). The SB latex latex (Dow DL 966, Tg 20°C) content was 12 parts in all coatings. All coatings

contained 1 part of CMC (Finnfix 10, Noviant Oy). The pH of the coating colors was adjusted to 8.5. The solids content of the coating colors was 63%.

UV and IR measurements

ATR-IR spectra were collected with an ATR objective attached to the Nic-Plan Microscope in a Nicolet 740 FT-IR spectrometer. The ATR objective had a ZnSe crystal. The spectra were collected in the wavenumber region from 4000 to 650 cm^{-1} by averaging 300 scans at a resolution of 8 cm^{-1}. The spectrum of the ZnSe crystal was used as the reference spectrum. The sample spot size in the ATR objective measurement was adjusted with a circular aperture to 100 micrometers.

UV measurements were performed with a CS 9000 Flying Spot Scanning Densitometer (Shimadzu Corp.). UV reflection-absorption spectra were measured over the wavelength range from 200 to 360 nm. The UV light source was a deuterium lamp, and the detector was a reflection photomultiplier. The sample spot size was 0.4 x 0.4 mm.

UV absorption at the wavelength of the SB latex band was collected as UV maps with a moving sample stage. One map consisted of three lines at 1 mm intervals. The length of each line was 10 mm. UV maps show how uniformly the latex is distributed in the x-y direction (Kline 1991).

Grinding method

A paper surface grinder was constructed to grind off surface layers from paper or board at 2-5 micrometer increments. The grinding technique is similar to the earlier surface grinder used at KCL (Hattula et al. 1978.) A paper sample (295 x 30 mm) is fastened to a moving metal sector, and a rotating cutter is pressed against the paper surface. The penetration depth of the rotating cutter is adjusted with a micrometer screw. The cutter and a paper sample fastened to the metal sector of the grinder are shown in Fig. 1.

Confocal Raman and photoacoustic IR measurements

Raman spectra were collected with a Kaiser HoloLab 5000 dispersive spectrometer using an excitation laser at a wavelength of 785 nm. The spectrometer was connected to a microscope. To reduce light scattering in the depth profiling measurements, the samples were treated with immersion oil. This technique is described in detail elsewhere (Vyörykkä 1999). The Raman spectra of the depth profiles were measured in incremental steps of 5 μm. The sample spot size was about 2-4 micrometers.

PA-FTIR spectra were collected with a Bio-Rad FTS 6000 FTIR spectrometer equipped with an MTEC 300 photoacoustic detector. Prior to analysis the photoacoustic cell was purged with helium. In rapid scan collection, 100-200 scans were co-added with a resolution of 8 cm^{-1} with moving mirror velocities from 2.5 to 20 kHz. The sample spot size was 1 mm.

Results and discussion

Surface sensitivity and depth profiling in ATR-IR and UV

The depth of IR light beam penetration into the coating in the ATR-IR measurements was estimated using thin coating layers on Mylar plastic film. Coatings containing SB latex and carbonate or SB latex and clay do not absorb IR radiation at 1710-1730 cm^{-1} (C=O stretching of ester linkage), where Mylar has a strong band.

The appearance of the ester band was studied in the ATR-IR spectra collected

from thin coating layers on Mylar film. The ester band due to the Mylar film was not seen in the spectra of coatings with thicknesses between 2 and 4 microns. This confirmed the assumption that ATR-IR spectra collected with a ZnSe crystal contain information from a 1-2 micrometer surface layer at wavenumber 1730 cm^{-1}.

Grinding of the paper surface removes coating layer material down to the depth set with the micrometer screw with a resolution of one micrometer. After grinding, the paper surface is somewhat rough, which may prevent good contact between the sample surface and the ATR crystal in IR measurement. The paper samples were therefore calendered before ATR-IR analysis. Combining paper surface grinding with ATR-IR measurement gives information on successive coating layers 2-3 μm in thickness.

UV spectrum of SB latex coating and surface sensitivity of UV measurement

SB latex absorbs strongly at around 260 nm. This band originates from aromatic double bonds in SB. The baseline of the SB absorption band is tilted differently in the clay and carbonate coatings, and it is therefore essential to define the baseline for the UV absorption band of SB latex separately for clay and carbonate based coatings.

The UV spectra of SB latex coatings were compared to the UV spectra of similar clay and carbonate coatings without latex, as shown in Fig. 2A and Fig. 2B. The coating containing only 100 parts clay pigment HG 90 and 1 part CMC (FF10) has some absorption in the UV spectrum around 260 nm, as shown in Fig. 2A. The carbonate coating containing 100 parts carbonate HC 90 and 1 part CMC does not have much absorption at wavenumber 260 nm, as shown in Fig. 2B.

Mylar film absorbs UV light as it contains aromatic structures similar to those in SB latex. The UV absorption maximum of Mylar film is at 290-300 nm. The appearance of the UV band originating from Mylar film in the spectrum of the latex-based coating was studied from the UV spectra of thin coating layers. It was found that UV light penetrated a clay/latex coating less than a carbonate/latex coating. In clay-SB the penetration was about 2 to 4 micrometers compared with 5 to 8 micrometers for a carbonate/latex coating. This experiment showed that UV measurement is not as surface sensitive as ATR-IR.

It is obvious that most of the UV absorption detected is from the upper part (1-2 μm) of the coating layer, but coating below the surface also has some effect on the absorption values obtained. However, this experiment gives only approximate UV light penetration depths. The thicknesses of thin coating layers were measured together with the rough plastic film below the coating. This causes some uncertainty in the coating layer thickness values obtained.

Surface sensitivity and depth profiling in confocal Raman and photoacoustic IR measurements

The depth resolution in confocal Raman measurement is usually determined from the step response curves, which are measured from a silicon wafer. In our Raman system, this depth resolution against the silicon wafer was measured to be approx. 5 μm, and the surface sensitivity for a single measurement was thus estimated to be half of that, i.e. approx. 2.5 μm. Determination of the depth resolutions theoretically and in different materials using confocal

Raman microscopy is dealt with in more detail elsewhere (Vyörykkä 1999). The confocal Raman technique gives information from depths similar to those measured with the ATR-IR technique.

The surface sensitivity of the photoacoustic IR technique was similar to that of the UV technique, i.e. approx. 4 μm, see Table 1. This thickness was obtained using rapid scan collection with a mirror velocity of 20 kHz. With lower collection velocities, the analysis depths were greater. Comparing the four techniques used here, the thickest coating layers can be measured with the photoacoustic IR technique.

The surface sensitivities of ATR-IR, UV, PAS-FTIR and Raman measurements in the coating layer are shown in Table 1.

Effect of pigment size on ATR-IR, UV, confocal Raman and photoacoustic IR spectra

SB latex content was measured from coatings having the same composition (100 parts pigment, 12 parts latex and 1 part CMC), but with different clay and carbonate pigment particle sizes. Since the latex content was the same in all coating colors, and the coatings were dried in the same way at room temperature, it was presumed that the samples would have uniform latex distributions. This was shown to be the case by analysing both sides of the calibration coatings.

IR bands representing pigment and latex bands were chosen from the regions were the pigment bands do not overlap the latex bands. In the clay coating, the band areas at 3619 cm^{-1} (OH in clay) and 1495 cm^{-1} (CH in SB) were calculated. In the carbonate coating, the band areas at 874 cm^{-1} (CO_3^{2-} in carbonate) and 760 cm^{-1} (CH in SB) were calculated. The IR spectra of the SB latex and of the pure clay and carbonate pigment are shown in Figs. 3A, 3B and 3C.

In ATR-IR spectra, the band areas originating from latex and pigment were somewhat dependent on pigment particle size. However, the latex/ pigment ratios calculated from the band areas were similar in coatings having different particle size pigments. Thus the latex/pigment ratio measured with ATR-IR was not affected by changes in particle size.

UV measurement showed different SB latex band heights as the pigment particle size changed. The SB latex absorption band height was much smaller in the coating made from larger particle size clay than in coatings having smaller clay particles. In carbonate coatings, the SB latex absorption band height was greatest in the coating containing the largest particle size carbonate, and the absorption decreased as the carbonate particle size decreased.

The UV results indicate that the signal collected by the detector in the UV measurement depends not only on the sample's UV absorptivity but also on the reflection properties of the surface layer. UV absorption results for samples having different particle sizes or different pigment shapes in the coating layer do not give comparable information on latex content without a separate calibration for each pigment type.

The experiment showed that changes in coating pigment particle size do not affect latex quantification with ATR-IR, but UV measurement is affected. The band areas calculated from ATR-IR

spectra and the UV absorbances are shown in Table 2.

In Raman measurements, the immersion oil sampling technique reduced light refraction and multiple reflections in coating layers, and thus no significant difference was seen in the latex/pigment ratios in samples with different particle sizes. However, pigment particle size affected the maximum light penetration into the sample. With the smallest pigment particles the amount of stray light was lowest, the result being greater penetration and collection depths (Vyörykkä 1999).

Earlier studies have shown that PA spectra are dependent on sample particle size (Garbassi et al. 1998). In the present study pigment particle size was also seen to affect the PA rapid scan spectra. The latex and pigment band areas were slightly different in coatings containing pigments with different particle sizes. The latex/pigment ratios determined by photoacoustic IR were, however, similar in clay and carbonate coatings. To take into account the effect of particle size in latex determination from PA spectra, the calibration sets should contain coatings with different particle sizes.

Latex concentration measurement

The calibration coating series included four pigment compositions, and in each series the SB latex content varied between 3 and 18 parts. The thicknesses of the coating layers released from the plastic film were from 25 to 35 μm. The upper and lower surfaces of the samples were analysed using three techniques: ATR-IR, UV and confocal Raman. Calibration curves were constructed separately for each pigment composition.

In traditional IR concentration analysis only absorbances at two chosen band positions are used to calculate band area ratio. In this study, the latex pigment ratio was determined from the ATR-IR spectra using multicomponent quantitative analysis with a Partial Least Squares (PLS) method. In the PLS calibration, all wavelengths registered are usually taken as variables. In this way all the information collected from the sample in IR measurement is used in the calibration.

The strongest bands in the mid-IR spectra of coatings are from pigments, and the pigment bands overlap some of the latex bands. Latex bands are of weak or medium intensity compared to pigment bands, as shown in the ATR-IR spectrum of a carbonate/latex coating in Fig. 4a. All the wavelengths registered from 4000 to 650 cm^{-1} were taken as variables for the PLS calibration. This diminished the effect of spectral noise and gave more information about the latex/pigment ratio in the coatings. A good correlation was found between IR spectra and latex content for both clay and carbonate coatings. The PLS model based on ATR-IR spectra of carbonate coatings explained 99% of the variance in the x-matrix and 97% of the variance in the Y-matrix using 8 components.

The PLS model based on the ATR-IR spectra of carbonate coatings was tested with external coating samples. The latex content in the external coating samples was 3, 6, 9, 12, 15 or 18 parts. The difference between the known and predicted amounts of latex obtained with the PLS model was 1 part or less. The results of PLS prediction from the ATR-IR spectra of carbonate coating samples not included in the calibration model are shown in Fig. 4b. The calibration model will be further developed for determination of the

latex/pigment ratio as base paper fibers appear after surface layer grinding.

Latex content measurement with UV was sensitive to changes in the latex content of coatings containing 100 parts of carbonate pigment. The sensitivity decreased as the carbonate content diminished. SB could not be measured from the coatings containing 100 parts of glossing clay. Two calibration curves for carbonate coatings (100 parts and 70 parts carbonate) containing between 3 and 18 parts of SB latex are shown in Fig. 6. Coatings with 100 parts fine clay (HG90) had higher gloss than the three coatings containing carbonate. Hunter gloss values for calibration coatings containing 12 parts latex are given in Table 3. It is likely that the higher reflectivity of the clay coating surface is responsible for the lower sensitivity in detecting the latex content with UV.

Both ATR-IR and UV measurements showed that the latex content was similar on both sides of the calibration coatings containing between 3 and 18 parts of latex. This indicates that no latex migration had occurred in the calibration samples.

In Raman measurements, determination of SB latex content was based on the determination of latex/carbonate ratios at all depths used in the analysis. Latex/carbonate ratios were determined by calculating the band heights of the respective compounds after the baseline correction. The baseline correction procedure was especially crucial in coatings containing kaolin clay due to the light-induced fluorescence effect of this material. This fluorescence made it impossible to measure coating compositions with 100 parts of clay. Two Raman spectra are shown in Fig. 7.

SB-latex carbonate ratios were determined by Raman spectroscopy from the upper and lower surfaces through the thick (around 30 μm) calibration coatings. The latex content was uniform throughout the coating layer in accordance with the ATR-IR and UV results.

Conclusions

The SB latex content of carbonate coatings was measured using the chosen techniques: ATR-IR, UV, and confocal Raman microscopy. In the case of clay-based coatings (100 parts HG 90), the SB latex content could be measured only with the ATR-IR technique. Fluorescence in the Raman analysis and high gloss in the UV analysis disturbed the measurements.

Depth profiling through the coating can be achieved with ATR-IR combined with surface grinding and confocal Raman with a 2-5 μm resolution. In PAS-FTIR measurements the z-directional analysis depth is about 4 μm when rapid scan collection at 20 kHz is used. With lower collection velocities the analysis depth is greater.

UV measures SB latex content in the surface layer, the thickness of which is between 2 and 8 μm. The analysis depth depends on pigment composition and coating structure.

Special attention must be given to those coating properties that influence SB latex determination. UV and PAS FTIR measurements are sensitive to changes in pigment particle size and shape. ATR-IR needs a smooth surface for good contact. In Raman measurements fluorescence interferes if the coating contains more than 50 parts clay.

Fig. 1. The paper surface grinder.

Fig. 2 A. UV spectra of an SB latex-clay-CMC coating and a clay-CMC coating.
Fig. 2 B. UV spectra of an SB latex-carbonate-CMC coating and a carbonate-CMC coating.

Fig. 3A. IR spectrum of SB latex.
Fig. 3B. IR spectrum of clay pigment.
Fig. 3C. IR spectrum of carbonate pigment.
Fig. 4A. ATR-IR spectrum of a carbonate-SB latex coating surface.

Fig. 4B. PLS prediction of SB latex content using the ATR-IR spectra of known coatings containing 100 parts carbonate.

Fig. 5. The UV calibration coatings containing carbonate-SB latex or clay/carbonate (30/70) SB latex.

Fig. 6A Raman spectrum of a carbonate-SB latex coating.
Fig. 6B. Raman spectrum of a clay/carbonate (50/50) SB latex coating.

Table 1. Surface sensitivity of carbonate and clay coating measurement using ATR IR, UV, Raman and PAS FTIR techniques.

Coating composition	**ATR IR**	**UV**	**Raman**	**FTIR/PAS rapid scan**
100 parts carbonate (HC 90) +12 parts SB latex (DL 966) + 1 part CMC (FF 10)	1-2 μm (at 1730 cm^{-1})	5-8 μm	Approx. 2.5 μm	approx. 4 μm (20 kHz, 1748 cm^{-1})
100 parts clay (HG 90) + 12 parts SB latex (DL 966) + 1 part CMC (FF 10)	1-2 μm (at 1730 cm^{-1})	2-4 μm	Measurement not possible due to fluorescence	approx. 4.5 μm (20 kHz, 1748 cm^{-1})

Table 2. ATR IR and UV measurement of SB latex from upper surfaces of clay and carbonate coatings: Pigment particle size varied.

CLAY SERIES: SB latex 12 parts, clay 100 parts and CMC 1 part			
Clay coating layer on a rough Mylar film	**ATR-IR band areas at 1495 and 3619 cm^{-1}**	**SB/pigment area ratio from ATR-IR spectra**	**UV absorbance of SB latex (top at 260 nm and base at 281-299 nm)**
LITHOPRINT (83%< 2 μm)	0.055 and 0.992	0.06	2.8
HG 90 (96% < 2 μm)	0.052 and 0.849	0.06	11.8
HG 92 (98% < 2 μm)	0.055 and 0.912	0.06	15.5
CARBONATE SERIES: SB 12 parts, carbonate 100 parts and CMC 1 part			
Carbonate coating layer on a rough Mylar film	**ATR-IR band areas at 760 and 874 cm^{-1}**	**SB/pigment area ratio from ATR-IR spectra**	**UV absorbance of SB latex (top at 257 nm and base at 288 nm)**
HC 60 (60% < 2 μm)	0.292 and 8.50	0.03	28.5
HC 90 (90% < 2 μm)	0.325 and 9.511	0.03	17.8
Setacarb (97% < 2 μm)	0.415 and 11.377	0.04	20.6

Table 3. Hunter gloss of uncalendered coating layer on rough plastic film.

Coating sample	Hunter gloss 75°, %
100 clay+12 SB+ 1 CMC	75.2
50 clay + 50 carbonate + 12 SB + 1 CMC	49.2
30 clay+ 70 carbonate + 12 SB + 1 CMC	42.1
100 carbonate + 12 SB + 1 CMC	25.8

Acknowledgements

The authors wish to thank the National Technology Agency of Finland, Tekes, for its financial support.

Literature

Eklund, D., Norrdahl, P., Heikkinen, M-L., (1995) Uneven ink absorption and its relation to drying of coated papers, Drying Technology 13 (4), 919.

Engström, G., Rigdahl, M., Kline, J., Ahlroos, J. (1991) Binder distribution and mass distribution of the coating layer - cause and consequence, Tappi Journal 74 (5), 171.

Engström, G. and Rigdahl, M. (1992) Binder Migration - Effect on printability and print quality, Nordic Pulp Paper Res. J. 7(2), 55.

Garbassi, F., Morra, M., Occhiello, E. (1998) Polymer Surfaces from physics to technology, John Wiley & Sons, England, p. 136.

Hattula, T., and Aschan, P.-E.(1978) Z-distribution analysis of binder in board coatings, Paperi ja Puu 60 (11), 665.

Häkkänen, H., (1998) Development of a method based on laser-induced plasma spectrometry for rapid spatial analysis of material distribution in paper coatings, Academic Dissertation for the Degree of Doctor of Philosophy, University of Jyväskylä, 60 pp.

Kim, L.H., Pollock, M.J., Wittbrodt, E.L., Roper, J.L., Smith, D.A., Stolarrz, J.W., Rolf, M.J., Green, T. J., Langolf, B.J. (1999) Reduction of back-trap mottle through optimization of the drying process for paper coatings, part I Tappi Journal 81 (8), 153.

Kline, J.E., Measuring binder migration with ultraviolet analysis (1991) Tappi Journal 74(4), 177.

Tomimasu, H., Ogawa, S., Sakai, Y., Yamasaki, T., Ogura, T. (1986) ESCA to analyze surface binder concentration of coated paper, TAPPI Coating Conference, May 4-5, Washington DC, 35-43.

Vyörykkä, J., (1999) Konfokaali-Raman-spektrometrin käyttö paperin päällysteen syvyyssuuntaiseen analysointiin Pro gradu-tutkielma, Fysikaalisten tieteiden laitos Oulun yliopisto, 74 s + liitt.

Wahls, M.W., Kenttä, E., Leyte, J.C. (2000) Depth Profiles in Coated Paper: Experimental and Simulated FT-IR Photoacoustic Difference Magnitude Spectra, Applied Spectroscopy 54 (2), 214.

Zang, Y.-H. ja Aspler, J.S.(1997) The effect of surface binder content on print density and ink receptivity of coated paper, 1997 TAPPI Advanced coating fundamentals symposium, 9-10 May, Philadelphia, PA, 165-170.

Zeyringer, E., Baure, W., Kovacic F., Ullrich, H., (2000) Einflüsse der Trocknung auf die Eigenschaftsenentwicklung holzfreied mehrfach gestrichener Papiere, Wochenplatt für Papierfabrikation 6, 356.

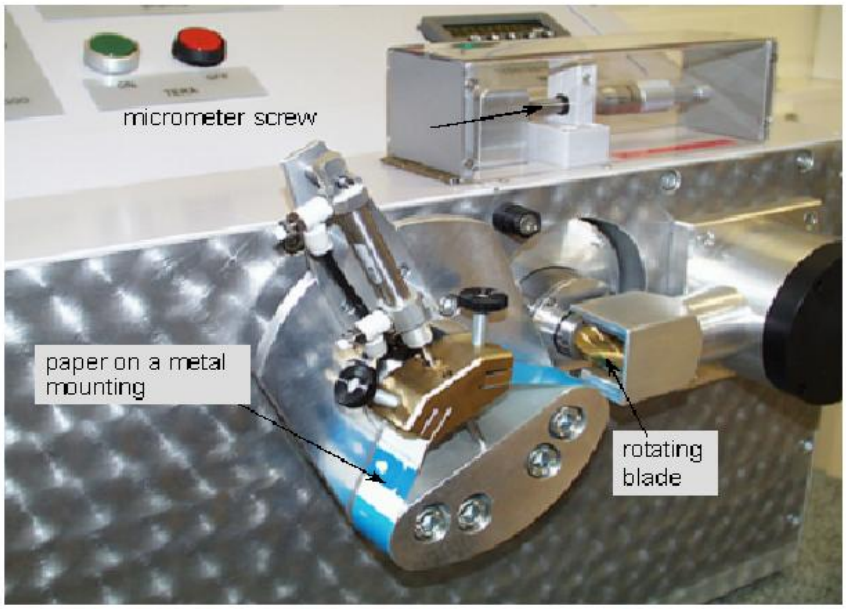

Fig 1. The paper surface grinder.

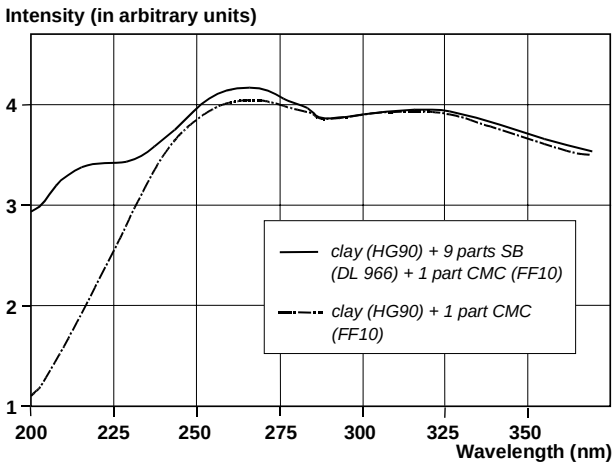

Fig. 2a. UV spectrum of an SB latex clay-CMC coating and a clay-CMC coating.

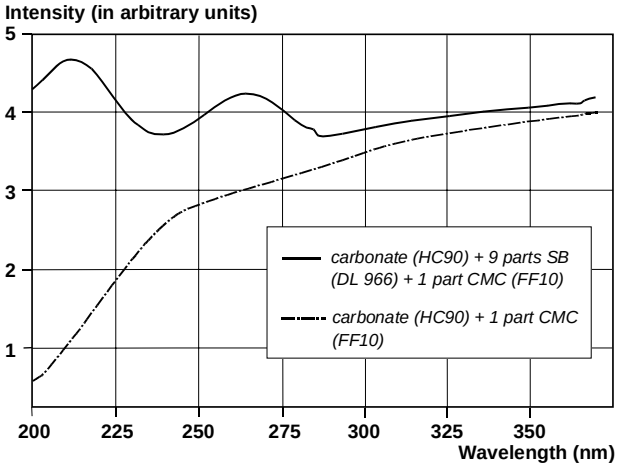

Fig. 2b. UV spectrum of an SB latex carbonate-CMC coating and a carbonate-CMC coating.

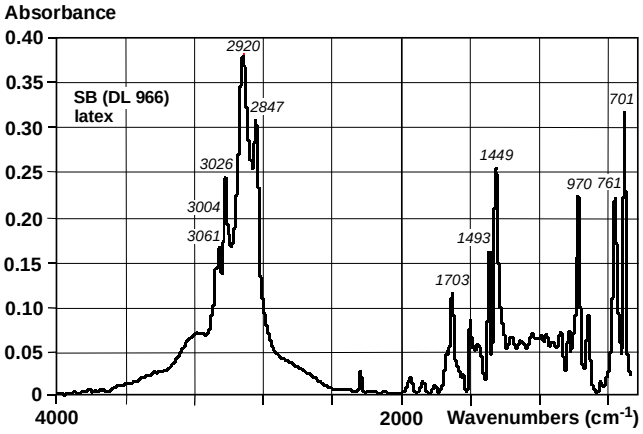

Fig. 3a. IR spectrum of an SB latex.

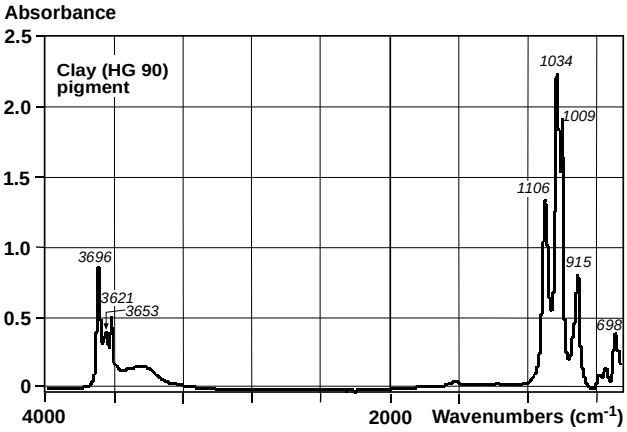

Fig. 3b. IR spectrum of a clay pigment.

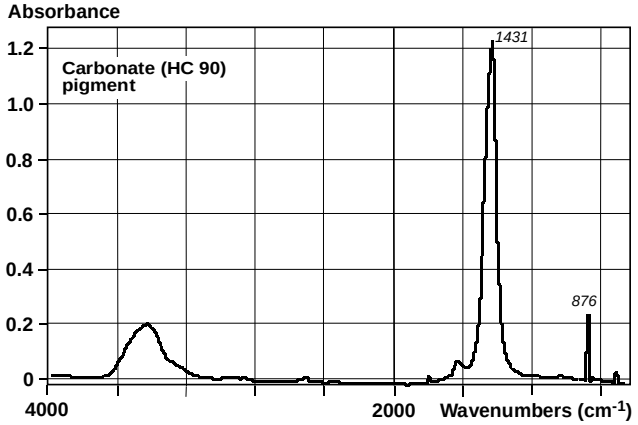

Fig. 3c. IR spectrum of a carbonate pigment.

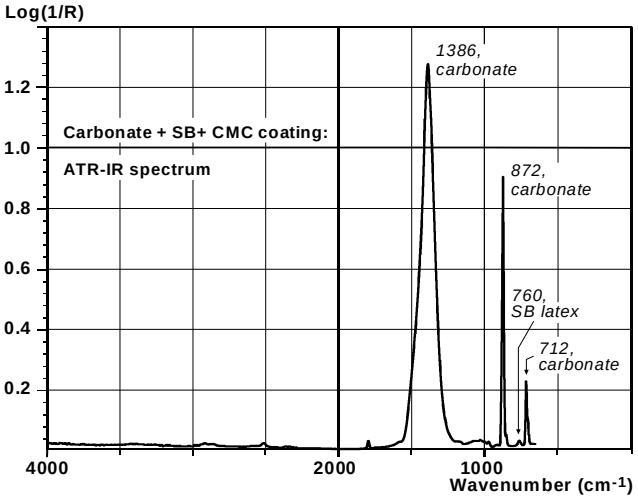

Fig. 4a. ATR-IR spectrum of a carbonate-SB latex coating surface.

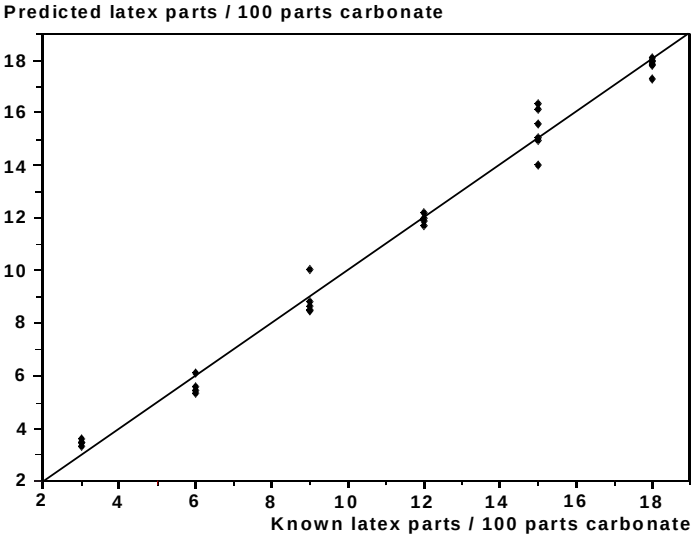

Fig. 4b

Fig. 4b. PLS prediction of SB latex content using the ATR-IR spectra of known coatings containing 100 parts carbonate.

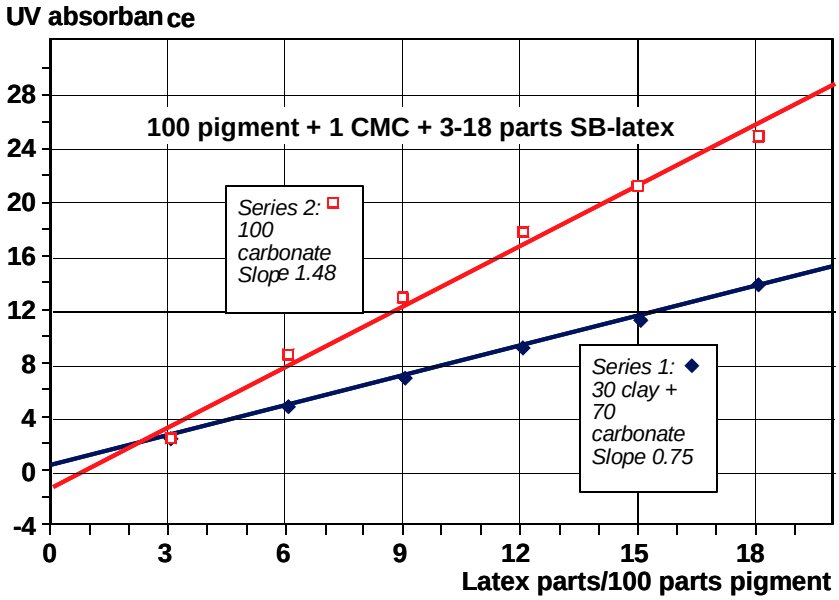

Fig 5. The UV calibration coatings containing carbonate-SB latex or clay/carbonate (30/70) latex.

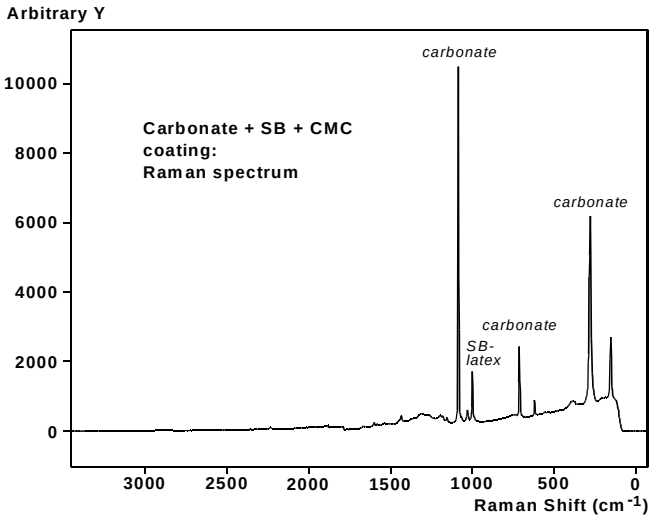

Fig. 6a. Raman spectrum of a carbonate-SB latex coating.

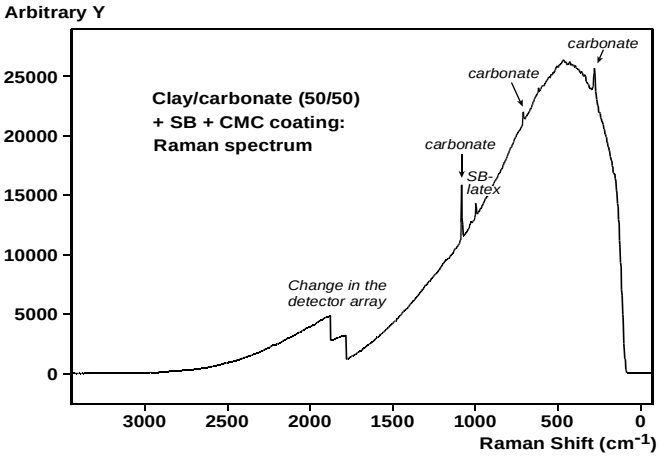

Fig. 6b. Raman spectrum of a clay/carbonate (50/50) SB latex coating.